Development 124, 2659-2670 (1997)
Printed in Great Britain © The Company of Biologists Limited 1997
DEV3660

TGFβ2 knockout mice have multiple developmental defects that are non-overlapping with other TGFβ knockout phenotypes

L. Philip Sanford[1], Ilona Ormsby[1], Adriana C. Gittenberger-de Groot[2], Hannu Sariola[4], Rick Friedman[3], Gregory P. Boivin[5], Emma Lou Cardell[6] and Thomas Doetschman[1,*]

[1]Departments of Molecular Genetics, Biochemistry and Microbiology, [3]Otolaryngology, [5]Pathology and Laboratory Medicine, [6]Cell Biology, Neurobiology and Anatomy, University of Cincinnati, Cincinnati, OH 45267, USA
[2]Department of Anatomy, Leiden University, Leiden, The Netherlands, [4]Institute of Biotechnology, University of Helsinki, Finland

*Author for correspondence (e-mail: thomas.doetschman@uc.edu)

SUMMARY

The growth and differentiation factor transforming growth factor-β2 (TGFβ2) is thought to play important roles in multiple developmental processes. Targeted disruption of the TGFβ2 gene was undertaken to determine its essential role in vivo. TGFβ2-null mice exhibit perinatal mortality and a wide range of developmental defects for a single gene disruption. These include cardiac, lung, craniofacial, limb, spinal column, eye, inner ear and urogenital defects. The developmental processes most commonly involved in the affected tissues include epithelial-mesenchymal interactions, cell growth, extracellular matrix production and tissue remodeling. In addition, many affected tissues have neural crest-derived components and simulate neural crest deficiencies. There is no phenotypic overlap with TGFβ1- and TGFβ3-null mice indicating numerous non-compensated functions between the TGFβ isoforms.

Key words: TGFβ2, gene targeting, heart defect, skeletal defect, epithelial-mesenchymal interaction, mouse, knockout

INTRODUCTION

TGFβ2 is a member of the highly conserved TGFβ super gene family that consists of more than thirty ligand proteins (reviewed by Kingsley, 1994). Members of this family represent structurally similar, yet functionally diverse growth factors which can regulate many aspects of cell behavior. TGFβ was originally named for its ability to promote anchorage-independent growth of fibroblasts in culture (Roberts et al., 1981) but it soon became clear that this peptide could either promote or inhibit cell growth depending upon the cell type examined and the presence of other growth factors. In general, TGFβs are mitogenic for cells of mesenchymal origin and inhibitory for cells of epithelial origin (Sporn et al., 1987; Massagué, 1990). Similarly, TGFβs also have dual activity with respect to modulating the differentiation of cells in vitro and in vivo.

TGFβs have the potential to modify cell migration, homing and location during development, through processes that are in part controlled by complex adhesive interactions between cellular receptors and components of extracellular matrix (ECM) (Massagué, 1990). Given all of these biological activities, it was anticipated that each of the TGFβ ligands would have widespread fundamental roles during embryonic development. Therefore, we and others have undertaken the genetic disruption of the three mammalian TGFβ isoforms to gain a better understanding of their function during development and in the adult (Shull et al., 1992; Kulkarni et al., 1993; Proetzel et al., 1995; Kaartinen et al., 1995).

TGFβ2 first appears in the preimplantation blastocyst (Slager et al., 1991) and its presence continues into adulthood (Miller et al., 1989). During embryogenesis, the TGFβ2 protein may be expressed uniquely in tissues or in the company of other TGFβs (Pelton et al., 1991). Sites of unique or predominant expression include: chondrocytes, osteocytes, precardiac mesoderm, cardiac myocytes, basement membranes of the kidney and gut, sensory epithelia of the eye and ear, perichondrial layers of facial cartilaginous tissues, as well as neural tissues of the spinal cord and peripheral nervous system (Pelton et al., 1991; Flanders et al., 1991; Millan et al., 1991; Schmid et al., 1991; Slager et al., 1991; Manova et al., 1992; Paria et al., 1992). In this paper, we show that TGFβ2 plays essential roles in the development of a wide range of tissues, including craniofacial, axial and appendicular skeleton, heart, eyes, ears, and organs of the urogenital tract.

MATERIALS AND METHODS

Generation of TGFβ2-null mice

A 62 bp oligonucleotide from mouse TGFβ2 exon 4 (Miller et al., 1989) was used to screen a genomic library derived from 129/J mouse DNA (Shull et al., 1992). A 4.7 kb *Sac*I fragment spanning exons 4 through 6 was subcloned from the phage DNA and ligated into pBluescript (Strategene). A poly(A)– pMC1neo cassette (Strategene) was blunt end ligated into the *Bam*HI site in exon 6. Next, the 3.5 kb targeting sequences containing 400 bp of 5′ homology, the neo cassette, and approximately 2 kb of 3′ homology were subcloned as a *Bam*HI-*Sac*I fragment into pBluescript. This plasmid was linearized with *Bam*HI and used to electroporate E14-1 ES cells as previously described (Shull et

al., 1992). The ES cells were selected using 400 mg/ml G418 for 7 days to identify stably transfected colonies. ES cell DNA was isolated using the method of Laird et al. (1991). Targeted colonies were initially identified by PCR amplification of a 1.5 kb fragment using an intron 5 primer, p5 (GCAGGGTCCTCTTTGTGAG) and a neo primer, pneo (GCCGAGAAAGTATCCATCAT). The amplification conditions were 35 cycles at 94°C for 30 seconds, 58°C for 30 seconds and 72°C for 1 minute. Southern blots were used to confirm homologous recombination. ES cells from two independent clones were microinjected into C57/Bl6J blastocysts by the ES cell transgenic core facility at the University of Cincinnati. Heterozygous and homozygous genotypes were detected with PCR using the exon 6 primers, p5 (AATGTGCAGGATAATTGCTGC) and p3 (AACTCCATAGATATGGGGATGC). The amplification conditions were 35 cycles at 94°C for 30 seconds, 57°C for 30 seconds and 72°C for 90 seconds.

Mouse strains

Blastocysts were prepared from C57Bl6J mice and the E-14.1 ES cells were derived from 129/Ola blastocysts. Male germ-line chimeras were bred to outbred Black Swiss females (Taconic) to produce F_1 offspring heterozygous for the *tgfβ2* locus. All animals used in the studies presented here were derived from these and succeeding F-generations of these mice. Animals derived from each ES cell line were bred and evaluated independently.

Inner ear preparations

E18.5 inner ears from fetuses were harvested and immersion fixed in 1% paraformaldehyde, 1% glutaraldehyde in phosphate buffer, pH 7.2. For light microscopy, inner ears were dissected and postfixed in buffered 4% OsO_4, dehydrated in ethanol and propylene oxide, and embedded in SPURR resin (Polysciences). Semithin sections (1-2 μm) were cut with a diamond knife and stained with 0.5% Toluidine blue in 0.5% sodium borate.

Anatomical and histological assessments

For skeletal staining, fetuses were skinned, fixed in 70% EtOH and eviscerated. After one week, the fetuses were further fixed for 1-2 days in acetone and then stained with Alcian blue and Alizarin red, following a modification of the method by McLeod (1980). All histology sections were stained with hematoxylin and eosin unless otherwise stated.

Gene expression measurements

The arrowheads in Fig. 1A represent the primers used for the screening of TGFβ2 message expression. Total RNA was prepared using the method of Chomczynski and Sacchi (1987) and cDNA was prepared as described in Sambrook et al. (1989). The presence of TGFβ2 message was determined using primers p5 and p3 as described above. The sequences of the β-actin control primers were upper: (GTCCCTGTATTGCCTCTGGTC) and lower: (TCGTACTCCTGCTTGCTGAT). The conditions for both of these reactions were the same as those used for genotypes above with the exception that the reaction for β-actin was for 25 cycles.

RESULTS

Targeted disruption of the TGFβ2 gene

The TGFβ2 gene consists of seven exons with the mature ligand coding region beginning late in exon 5 and ending in exon 7. A targeting vector containing 3.5 kb of homology was constructed to ablate the mature ligand coding region by insertion of the neomycin resistance (neo^R) gene into exon 6 (Fig. 1A and Materials and Methods). The 5′ region of the neo^R gene contains translation stop codons in all three reading frames resulting in a targeted locus that codes for a truncated peptide (32 amino acids into the mature peptide) thereby preventing synthesis of any full-length mature peptide dimers. If exon 6 containing the neo cassette is spliced out of the mature peptide it will cause (1) the loss of 51 amino acids, (2) an immediate frameshift mutation in exon 7 and (3) a grossly aberrant mature peptide of only 15 amino acids in length. Potentially targeted ES cell lines were tested by Southern blotting. Four independently targeted embryonic stem (ES) cell clones were obtained (Fig. 1B) and two were used to produce germ-line chimeras via blastocyst injection. The genotype of a representative litter is shown in Fig. 1C. These data were confirmed with Southern blotting (not shown). Reverse transcriptase polymerase chain reaction (RT-PCR) analysis of biologically essential exon 6 sequences detected no wild-type (WT) message in the TGFβ2-null mice (Fig. 1D).

Null mice are born with congenital cyanosis

Mice heterozygous for the TGFβ2-null allele present no apparent defects. No significant embryonic lethality was observed. In contrast, the birth weights of E18.5 Cesarean-derived TGFβ2-null fetuses are 12% less than their wild-type littermates (1.17±0.14 g, n=31 compared to 1.32±0.15 g, n=31, P<0.005). The phenotypes of TGFβ2 knockout mice derived from both targeted ES cell lines were identical.

Two-thirds of the TGFβ2-deficient mice die shortly before or during birth and the remainder are born cyanotic. The live-born pups are responsive to mechanical stimulation but exhibit respiratory distress and routinely die within minutes. Congenital cyanosis can ensue from impaired cardiovascular function,

Table 1. Congenital heart defects in null mutants

Phenotype	Penetrance
Lung-postnatal	
Dilated conducting airways	5/5
Collapsed terminal and respiratory bronchioles	5/5
Heart defects	
Ventricular septum defects	15/16
Dual outlet right ventricle	3/16
Dual inlet left ventricle	4/16
Skeletal defects	
Occiptital bone	16/16
Parietal bone	16/16
Squamous bone	16/16
Palatine bone (cleft palate)	7/32
Alisphenoid bone	16/16
Mandibular defects	16/16
Shortened radius and ulna	16/16
Missing deltoid tuberosity and third trochanter	15/16
Sternum malformations	4/16
Rib Barreling	15/16
Rib Fusions	2/16
Spina bifida	16/16
Ocular hypercellularity and reduced corneal stroma	4/4
Inner ear defects	4/4
Urogenital defects kidney	10/10
Dilated renal pelvis	3/10
Agenesis (females only)	1/5
Uterine horn ectopia	2/5
Testicular ectopia	5/5
Testis hypoplasia and vas deferens dysgenesis	1/5

All data above is from E18.5 TGFβ2-deficient animals.

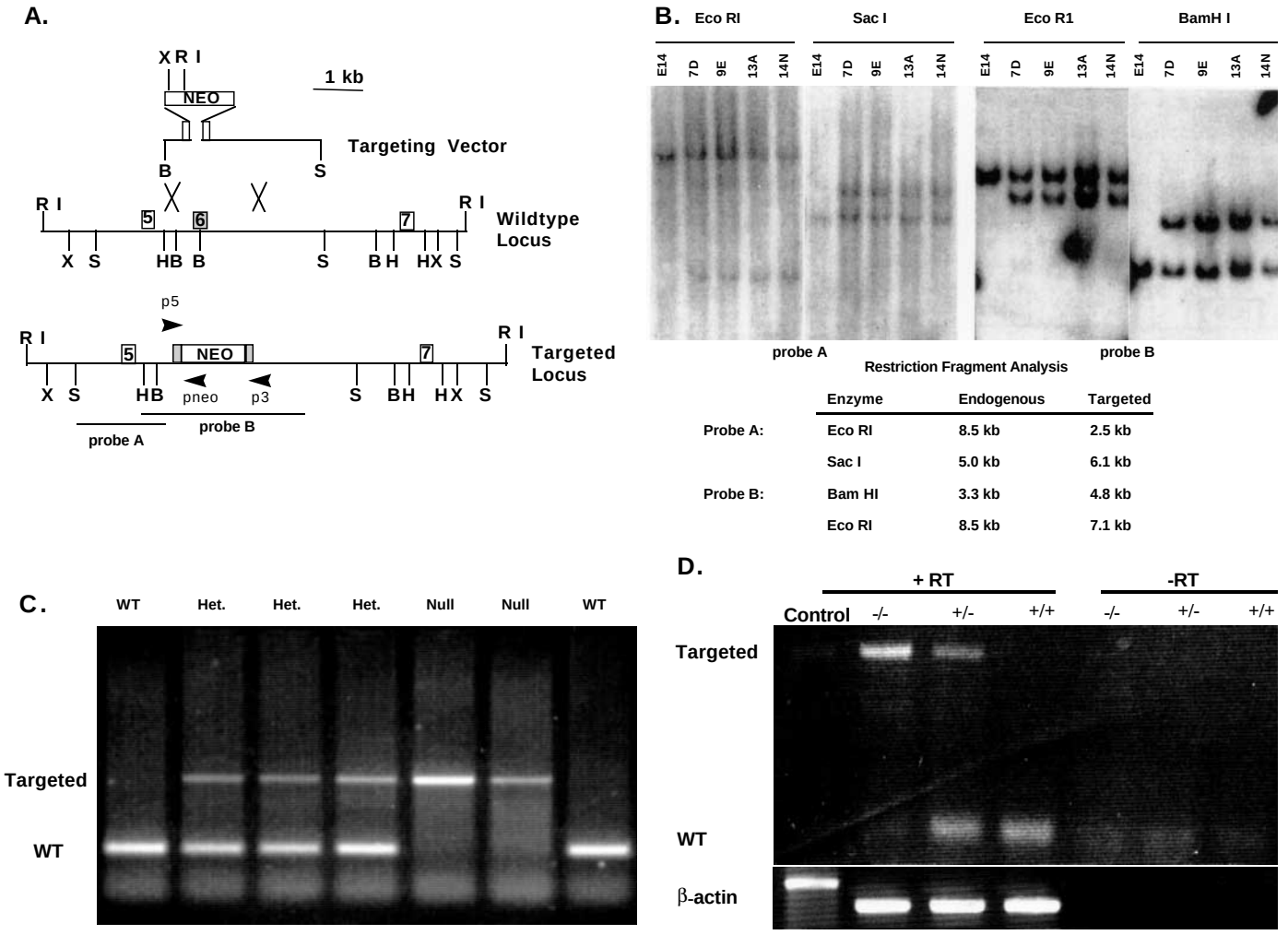

Fig. 1. Targeting of the mouse TGFβ2 gene. (A) Diagrams of the wild-type locus, the targeting vector and the predicted targeted allele. Shown is the exon structure and the primers used for various PCR reactions to distinguish the targeted from the wild-type alleles in both ES cell and tail clip DNA. Abbreviation used: B, *Bam*HI; E, *Eco*RI; H, *Hin*dIII; S, *Sac*I; X, *Xba*I; neo, poly(A)$^-$ pMC1 neo cassette. (B) Southern blots of ES cell DNA showing both control cell DNA (E14) and targeted clones. DNA was digested with the enzymes indicated and probed with either probe A or probe B. Expected restriction fragments are listed. (C) PCR-genotype of the offspring from a heterozygote (HET) intercross. The null (1.3 kb) and the wild-type (132 bp) alleles are amplified using primers p3 and p5. (D) RT-PCR analysis from HET, wild-type and null animals showing the absence of detectable TGFβ2 exon 6-specific message in the null animals. +RT and –RT represent PCR substrates produced in the presence or absence of reverse transcriptase. The β-actin lanes are PCR controls for genomic DNA contamination. The β-actin control lane is genomic DNA only.

pulmonary insufficiency or neuro-muscular defects in the respiratory system. Since several studies have reported that TGFβ2 is expressed in the developing mouse lung (Millan et al., 1991; Pelton et al., 1991; Schmid et al., 1991), we performed a histological examination of the lungs. Prenatal E18.5 lungs from null animals have no gross morphological defects that were considered incompatible with postnatal survival. However, examination of postnatal lungs revealed collapsed conducting airways (data not shown).

Congenital heart defects

Transverse sections of one representative null heart revealed a large number of structural defects as shown in Fig. 2. At the arterial outflow level, a section from a wild-type heart shows the continuity of the pulmonary trunk and pulmonary arteries (Fig. 2A). In the null littermate, the ascending aorta is comparatively small and thin walled, or hypoplastic (Fig. 2B). At the level of the outflow tract below the truncus arteriosus, the normal heart shows the configuration of the pulmonary valve and the orifice contacting the right ventricle. The aorta is in a right posterior position and does not show the orifice level (Fig. 2C). In the null embryo (Fig. 2D), the aortic and pulmonary orifices are both above the right ventricle. Both show valve leaflets (arrow) that are patent (aortic valve leaflet patency is not shown; an example of pulmonary patency is seen in Fig. 2A). At this developmental stage, the normally muscular outflow tract septum (Fig. 2C) is mesenchyme in the null heart (Fig. 2D, arrow). At the level of the atrioventricular valves, the normal heart shows separation of the tricuspid orifice and valve from the mitral orifice and valve (Fig. 2E). In the null embryo, both tricuspid and mitral valves are connected to the left ventricle (Fig. 2F).

A large ventricular septal defect is present between the double inlet left ventricle and the double outlet right ventricle. The myocardium is hypercellular and less trabeculated, and there is an enlarged right ventricle. An atrial septal defect is found in a small percentage of mutant animals (not shown). None of these congenital heart defects appear at full penetrance in the null mutants (Table 1) rather, all of the null hearts display a subset of these defects.

A number of unrelated heart pathologies have been associated with hypothyroidism (reviewed in Polikar et al., 1993). These include DeGeorge and CATCH-22 syndromes. Histological examinations of the thyroid and parathyroid glands of TGFβ2-null mice revealed no anomalies (data not shown).

Craniofacial defects

Since most TGFβ2-null mice show retrognathia and dysmorphic calvaria, (by gross appearance) skeletal preparations were made from day E18.5 mice. As shown in Fig. 3A-E, a general reduction in bone size and cranial ossification was seen. This form of dysgenesis was seen in the frontal, interparietal, parietal and squamosal bones. These bone morphogenetic deficiencies produced enlarged fontanels. This pattern of reduced ossification is not consistent with delayed development as seen in a comparison with a wild-type E17.5 skull (Fig. 3F). Also, there is nearly complete agenesis of the alisphenoid and occipital bones (Fig. 3B,D).

Similarly, the mandibles from the TGFβ2-null mice have a number of morphologic defects. The angle of the null mandible is always absent and the coronoid and condyloid processes are consistently diminished to approximately one-half their normal dimensions (Fig. 3E). Additionally, the mandibles are smaller and the masseteric ridge is more pronounced with more anterior and dorsal displacement when compared to the wild-type mandible. All of the craniofacial defects described above were fully penetrant in mice derived from both targeted ES lines.

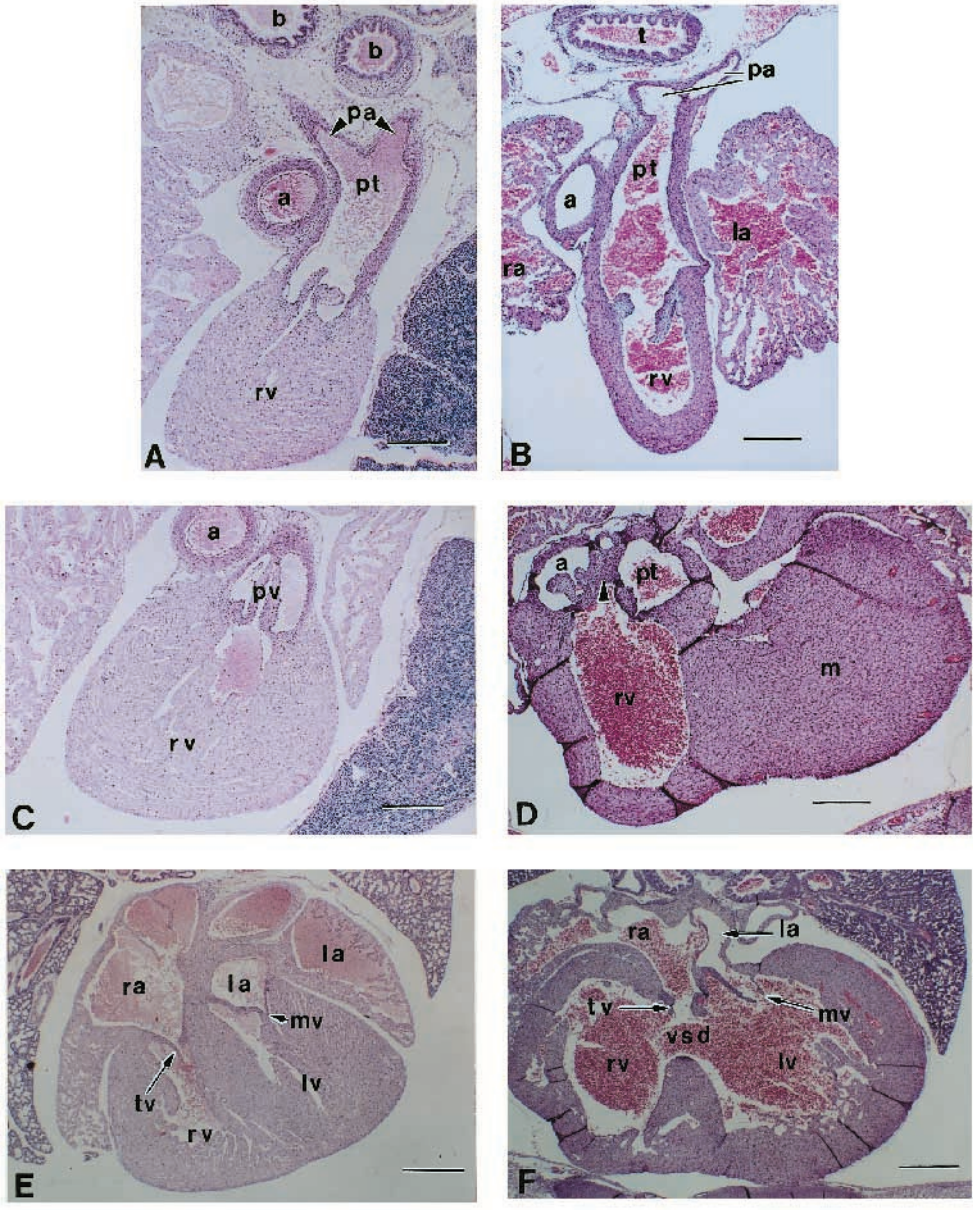

Fig. 2. Congenital heart defects of TGFβ2-null mice. Transverse heart sections at the arterial (A,B), outflow tract (C,D) and atrioventricular valve (E,F) levels of day E18.5 of null mutant (A,C,E) and wild-type littermate (B,D,F) mice. (A) Arterial level section of normal heart showing comparable arterial wall thickness between the pulmonary trunk and the aorta. Abbreviations: a, aorta; b, bronchus; pa, pulmonary arteries; pt, pulmonary trunk; rv, right ventricle. Bar, 120 μm. (B) Arterial level section of a null heart showing a hypoplastic aorta vessel wall. Abbreviations: la, left atrium; ra, right atrium; t, trachea. Bar, 120 μm. (C) Right ventricular outflow tract level of normal heart. Abbreviation: pv, pulmonary vein. Bar, 120 μm. (D) Right ventricular outflow tract level of mutant heart showing mesenchymal septum. Abbreviation: m, myocardium of the left ventricular wall; arrow, mesenchymal outflow tract septum. Bar, 120 μm. (E) Atrioventricular valve level section of normal heart showing a normal ventricular septum. Abbreviations: lv, left ventricle; mv, mitral valve; tv, tricuspid valve. Bar, 200 μm. (F) Atrioventricular valve level section of mutant heart showing a large ventricle septum defect. Bar, 200 μm.

Cleft palate

Fig. 3B,H and J shows the extensive cleft palate seen in 23% of the TGFβ2-null animals. The defect was always a complete anteroposterior cleft of the secondary palate, leaving the nasal septae exposed, and extending to the soft palate as well. There was no fusion of the primary palate to the secondary palate and no primary palate cleft or cleft lip was ever observed. These cleft palates had defects not only in the palatine shelves of the maxillary bone but also in the formation of the pterygoid process of the basisphenoid bone (Fig. 3B). Histological analysis of these animals at day E18.5 shows a failure of the palatal shelves to elevate into a horizontal orientation for the process of apposition (Fig. 3I,J). This phenotype is the only craniofacial defect that is not completely penetrant.

Non-cranial skeletal malformations

Neonatal mice are born with a form of limb laxity in which both forelimbs and hind limbs appear rotated and extended toward the midline. An analysis of the forelimb bones reveals an absence of the deltoid tuberosity on the humerus (Fig. 4A) and the analogous third trochanter on the femur (Fig. 4B). The radius and ulna, are consistently shortened when compared to wild-type limbs (Fig. 4A). Similarly, a reduction in the size and development of the olecranon process of the ulna is observed. These limb defects were fully penetrant.

TGFβ2-null mice present with spina bifida occulta. Fig. 4D shows that the vertebrae in the thoracic and lumbar regions have defects in the closure of the neural arches. The arches are formed but fail to fuse at the midline of the neural tube as seen in the wild-type animals (Fig. 4C). The typical range of this defect is from the 10th thoracic vertebra to the 5th caudal vertebra.

Sternum and rib defects were observed in some of the null animals (see Fig. 4F; Table 1). The sternum malformations included: bifurcation, incomplete manubrium and vestigial xiphoid process. The most prominent rib defect occurring in

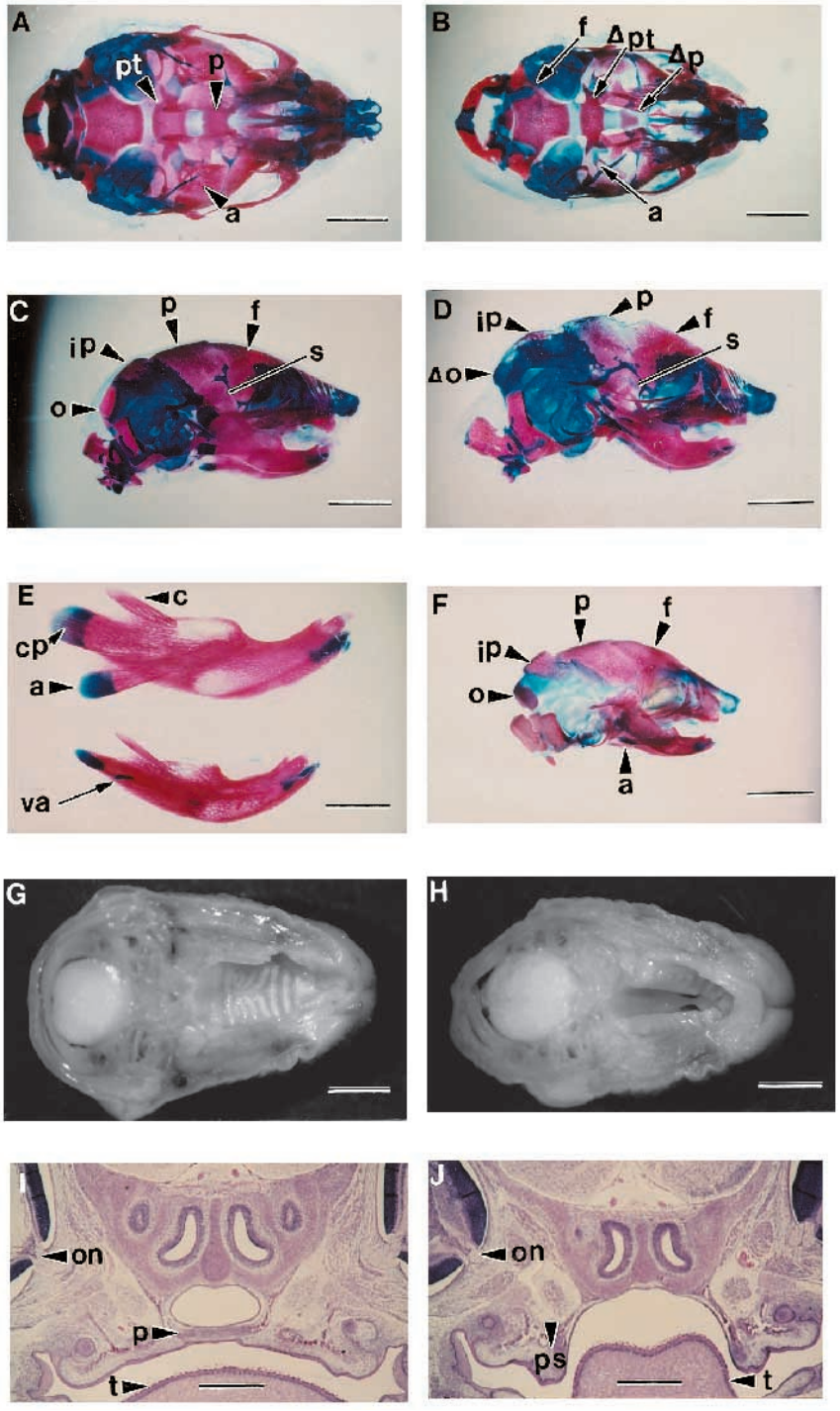

Fig. 3. Craniofacial defects of TGFβ2-null mice. (A) Ventral view of alcian blue (cartilage) and alizarin red (bone) staining of E18.5 skull from sibling wild-type animal. Abbreviations: a, alisphenoid; p, palatine bone; pt, pterygoid bone. Bar, 2.2 mm. (B) Ventral view of null sibling skull with cleft palate showing generally reduced ossification and the absence of the alisphenoid, pterygoid process and palatine bones. Abbreviations: f, fusion of exoccipital and basisphenoid bones; Δp, deleted palatine bone; Δpt, deleted pterygoid process. Bar, 2.2 mm. (C) Lateral view of wild-type E18.5 skull. Abbreviations: f, frontal bone; ip, interparietal bone; o, occipital bone; p, parietal bone; s, squamous bone. Bar, 2.2 mm. (D) Lateral view of null E18.5 skull showing reduced ossification of the interparietal, occipital, parietal, frontal and squamous bones. Abbreviations: Δo, deleted occipital bone. Bar, 2.2 mm. (E) Mandibles from E18.5 siblings. Abbreviation: a, angle; cp, condylar process; c, coronoid process; va, vestigial angle. Bar, 1.36 mm. (F) Lateral view of E17.5 skull from a HET animal used as a less mature growth control for A-D above. Bar, 2.2 mm. (G) Palate from a wild-type E18.5 mouse. Bar, 2.2 mm. (H) Cleft palate from a null E18.5 mouse. Bar, 2.2 mm. (I) Transverse histology section of wild-type E18.5 palate. Abbreviations: on, optic nerve; p, palate; t, tongue. Bar, 550 μm. (J) Transverse histology section of a sibling null E18.5 mouse with cleft palate showing vertical palatal shelves (ps). Bar, 550 μm.

nearly all of the animals examined involved abnormal curvature of the ribs which contributed to 'barrel chest.' This malformation forms a larger more rounded pulmonary cavity when viewed in transverse section. Similarly, the clavicles of the null mice consistently display ventral curvature (Fig. 4G). Finally, wavy irregular ribs or fused ribs were seen in one-third of the null animals (data not shown).

Eye developmental defects

All TGFβ2-null mice examined have a hypercellular infusion in the posterior chamber of the eye (see Fig. 5A,B). These structures contain many mitotic figures, are composed of isolated melanocytes, neuronal cells and mesenchymal cells, and are vascularized. Similarly, both the inner and outer neuroblastic layers of the retina appear hyperplastic. Additionally, the corneal stroma is approximately one-third as thick as in wild-type animals (see inset, Fig. 5C,D).

Inner ear defects

The spiral limbus is a condensation of mesenchyme that extends outward from the cochlear modiolus. This structure and the overlying epithelium (the interdental cells) are well developed in the E18.5 day wild-type mouse (Fig. 5E). The null mutants fail to form the spiral limbus in the basal cochlear turn by this time (Fig. 5F). The spiral ganglion is normally separated from the sensory organ of Corti by the intervening spiral limbus. The afferent nerve fibers travel this distance through Rosenthal's canal at the base of the spiral limbus. The spiral ganglion of the mutant lies close to the sensory epithelium as the result of the absent limbus and Rosenthal's canal (not shown). The interdental cells overlying the spiral limbus appear undifferentiated in the null animal.

The scala vestibuli of the mutant cochlea is only partially canalized with incomplete dissolution of the mesenchyme and poor organization of the mesothelial surface of Reissner's membrane, the partition between the perilymphatic space of the scala vestibuli and the endolymphatic space of the scala media. In addition, the greater epithelial ridge with its basal lamina is separated from the underlying basilar membrane in the mutant ears. These defects are present in all of the null animals examined.

Urogenital defects

Ten TGFβ2-null animals were examined for urogenital development and all but one possessed one or more anomalies (see Fig. 6; Table 1). All males showed abnormal urogenital development by displaying testicular ectopia. One male had an enlarged renal pelvis and another developed unilateral testicular hypoplasia with lack of an epididymis and concomitant vas dysgenesis (Fig. 6B). Two of five females showed an analogous ectopia of the uterine horns by a ventral displacement with respect to the kidneys (not shown). Three of five females had no obvious abnormalities of the uteri or ovaries; and showed some degree of kidney abnormality, including agenesis and dialated renal pelvis. When null kidneys are formed in females, tubulogenesis occurs, but is followed by dysplastic changes manifested by progressive dilatation of the renal tubules, degeneration of the tubular epithelium, proteinuria in the lumen of the tubules and enlargement of the renal pelvis (Fig. 6D,E). One female showed adrenal ectopia (not shown).

Other organs

The brain, gut and tooth bud are other likely sites for development defects based on embryonic TGFβ2 expression studies (Pelton et al., 1991; Millan et al., 1991; Schmid et al., 1991). Histological examination of these tissues from day E18.5 mice revealed no overt pathologies (not shown).

DISCUSSION

TGFβ2-deficiency during mouse gestation is manifested in multiple developmental defects affecting a wide range of organs including: the heart and outflow tract; craniofacial, axial and appendicular skeletal elements; multiple eye and inner ear mesenchyme abnormalities; and the urogenital system (summarized in Table 1). These defects are coincident with the TGFβ2 expression data and suggest a role for this growth factor in epithelial-mesenchymal transformations. Furthermore, these data show that TGFβ2 isoform (in contrast to TGFβs 1 and 3) is essential in many processes of normal embryonic and fetal development in the mouse.

Null mice die from congenital cyanosis

Analysis of the lungs of TGFβ2 knockout mice suggests a small reduction in the volume of distal saccules just before birth, and collapsed distal airways with dilated conducting airway passages in live-born mice. This is consistent with the expression of TGFβ2 and the TGFβ receptors in the developing mouse lung (Pelton et al., 1991; Barnett et al., 1994).

In agreement with the predictions of Dickson et al. (1993), the TGFβ2-null mouse develops numerous congenital heart disorders. There is a growing body of evidence that many heart defects can be the result of mutations in single genes (reviewed in Payne et al., 1995; Rossant, 1996). We believe that the heart defects present in the null mice are likely to cause the prenatal lethality that affects two thirds of the null animals, and that they contribute, along with pulmonary insufficiency, to the postnatal lethality of the remaining one third of the TGFβ2-null animals. We have observed that E12.5-E14.5 null hearts beat and circulate blood, which conforms with the null animal's survival to perinatal stages and with reports that failure of embryonic circulation is lethal in utero between days E10 and E16 (Copp, 1995; Sukov et al., 1994).

Cardiovascular development

A deficiency in migration, homing, or maturation of cranial neural crest cells in the presumptive head and heart regions is consistent with the craniofacial and cardiac outflow septum defects in the TGFβ2 knockout animal (Besson, 1986, Le Douarin et al., 1993). TGFβs have been shown to modify neural crest cell (NCC) differentiation and mitogenesis in vitro (Rogers et al., 1992; Howard and Gershon, 1993; Leblanc et al., 1995). Also, TGFβs are known to play important roles in modulating the production of both ECM components and cell adhesion molecules, which are thought to be essential for NCC migration and homing (Massagué, 1990; Erickson and Perris, 1993).

Lineage analysis studies by Le Lievre and Le Douarin (1975) established that the avian aortic tunica media is composed of smooth muscle cells derived from two different developmental lineages. One arises from cardiac neural crest

and has an ectodermal origin. The other is derived from lateral mesoderm and consists of local mesenchymal cells that surround and invest the developing outflow tract elastic arteries (Le Lievre and Le Douarin, 1975, Rosenquist and Beall, 1990). Recently, Topouzis and Majesky (1996) reported that the smooth muscle in the cardiac outflow tract is derived from two distinct developmental sources distinguished by differential responsiveness to TGFβ1. The mesenchyme-derived smooth muscle cells (SMC) are inhibited by TGFβ1 in culture; whereas, the neural crest-derived SMC are stimulated to divide by TGFβ1 in culture. Therefore, it is plausible that TGFβ2 may actually be this signal instead of TGFβ1 and that the TGFβ2-null animals fail to provide this mitogenic signal to the aorta resulting in SMC hypoplasia in this region.

Retroviral tracing shows that NCC reach the endocardial outflow tract ridges, which are essential in outlet septation (Noden et al., 1995). While problems with SMC growth could lead to the thinning of the aortic wall, reduced mesenchymal neural crest contribution to the outflow tract could lead to sub-optimal interaction of cushion tissue and outflow tract myocardium, resulting in the null animal's fibrous outflow tract septum instead of a normal myocardial septum. Defects in outflow tract septation combined with an improperly looped heart tube would lead to a right-sided aorta and dual outlet, right ventricle (Fig. 2D). A misalignment of the outflow tract septum and the main body of the ventricular septum would lead to the ventricular septum defects seen in the null hearts. In the most extreme cases, the tricuspid orifice is not positioned over the right ventricle and this leads to dual inlet, left ventricle (Bouman et al., 1995) as seen in Fig. 2F.

Skeletogenesis

During craniofacial chrondrogenesis, there is an essential inductive interaction between the first pharyngeal arch neural crest-derived mesenchyme and the head epithelium, which must occur to initiate the chondrogenic process (Nichols, 1981; Hall, 1982). Most of the affected bones in the skull, with the exception of the occipital are derived from first pharyngeal arch crest cells (Noden, 1991; Couly et al., 1993). Cellular condensations precede these chondrogenic events. These occur through either increased mitotic activity or cellular aggregation. The aberrant skeletogenesis observed in the TGFβ2-null animals suggests that at least one of the above steps is compromised.

The TGFβ2 knockout mice have a number of non-craniofacial skeletal abnormalities including limb, rib and spinal defects, indicating that a single locus defect can cause both axial and appendicular skeletal malformations. Several features of the diverse skeletal defects in the null mice are worthy of mention. First, most of the skeletal anomalies were manifested by size reductions of normal tissues, which indicates a role of TGFβ2 in skeletal induction and growth. Exceptions to this general diminution in size were the absence of the angle of the mandible, the occipital and the alisphenoid bones. The angle of the mandible may have been developmentally relocated to a more lateral position (see vestigial angle in Fig. 3F). These observations imply a role for TGFβ2 in skeletal patterning. Long bones were also affected, which are produced by endochondral rather than membranous ossification, as are the bones in the skull, clavicle and spine. These data support a role for TGFβ2 in both of these chondrogenic pathways.

Eye and ear development

Numerous epithelial-mesenchymal interactions take place during normal eye development (reviewed in Tripathi et al., 1991; Barishak, 1992). TGFβ2 expression has been found in several regions of the eye (Pasquale et al., 1993; Lutty et al., 1993; Nishida et al., 1995). In the null animals, the corneas develop with a reduced stromal layer. This is consistent with TGFβ's established role in promoting ECM deposition (Massagué, 1990). Elsewhere in the eye, hypercellularity of the posterior chamber appears to result from persistence of the vascular tunic which is normally eliminated before birth (Pei and Rhodin, 1970). It is possible that this structure and the hypercellular neuroblastic layers could have arisen from aberrant mitogenesis of resident cells or a failure in TGFβ2-mediated apoptosis to eliminate these cells. These data indicate a direct role of TGFβ2 in normal eye remodeling.

Although reciprocal interactions between the epithelium and mesenchyme of the developing inner ear are presumed to occur, the molecular bases for these interactions are poorly understood. Tissue culture and auditory explant experiments have demonstrated the inductive influences of the cochlear epithelium on the periotic mesenchyme and those of the mesenchyme on the epithelium. For example, periotic mesenchyme cultured without cochlear epithelium fails to condense in preparation for otic capsule formation (Van de Water, 1981; Frenz et al., 1992). The developmental cochlear abnormalities identified in the null animals suggest TGFβ2 plays a critical role in the epithelial-mesenchymal interactions occurring during cochlear morphogenesis. This conclusion is further supported by limited surveys of TGFβ expression in the mouse embryo localizing TGFβ2 mRNA in the developing cochlear epithelium and TGFβ2 peptide in the underlying mesenchyme (Pelton et al., 1990, 1991). The TGFβ2 null animals fail to show mesenchymal condensation in the spiral limbus and differentiation of the overlying interdental cells. These data and the incomplete canalization of the scala vestibuli suggest that TGFβ2 plays an important paracrine role in guiding epithelial and mesenchymal differentiation and patterning in the inner ear. Although a complete understanding of the function of the spiral limbus and interdental cells is lacking, the former demonstrates a significant Na^+/K^+-ATPase activity suggesting a role in cochlear fluid homeostasis and the latter may be involved in secretion of some of the components of the tectorial membrane (Zuo et al., 1995; Nakazawa et al., 1995). Lastly, the separation of the greater epithelial ridge from the basilar membrane suggests a defect in adhesion which may result from either defective ECM production or the absence of appropriate cell adhesion molecule expression.

Urogenital development

Our initial studies suggest that, with the exception of females missing one kidney, the early phases of kidney induction occur normally and result in tubulogenesis. Consistent with reports of TGFβ2 expression in the kidney tubules and basement epithelium (Pelton et al., 1991), it appears that some signal is missing in female null animals which maintains normal kidney development. In the absence of TGFβ2, normal renal tubulogenesis occurs until around E15.5. At this point, a deficiency in TGFβ2 leads to a progressive deterioration of the kidneys, as suggested by the degenerating tubular epithelium, the presence of protein casts

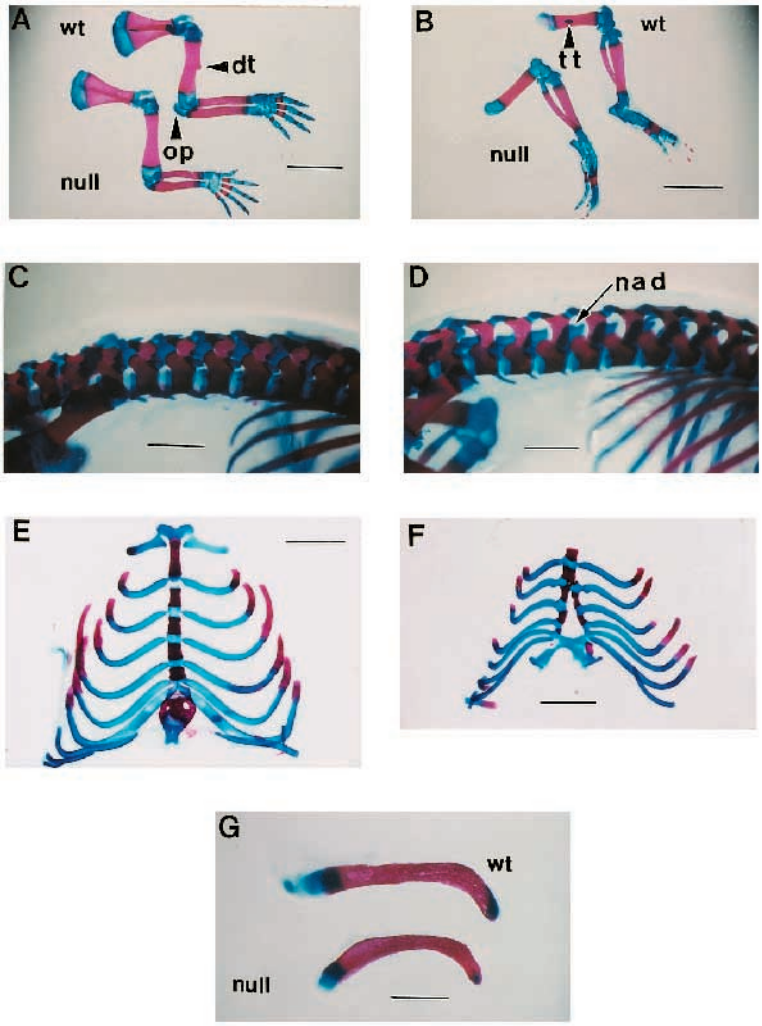

Fig. 4. Trunk and limb skeletal defects from the TGFβ2-null mice. (A) Forelimbs from E18.5 wild-type (top) and null (lower) siblings showing missing deltoid tuberosity (dt), reduced olecranon process (op) and shortened radius and ulna in null limb. Bar, 2.7 mm. (B) Hindlimbs from E18.5 wild-type (top) and null (lower)siblings showing extended foot and absent third trochanter (tt) in the mutant limb. Bar, 2.7 mm. (C) Spinal column from wild-type E18.5 mouse showing normal neural arches from a dorsal-lateral aspect. Bar, 1.4 mm. (D) Spinal column from E18.5 null sibling mouse showing the neural arch defect (nad) from a dorsal-lateral aspect. Bar, 1.4 mm. (E) Ventral rib cage from a wild-type E18.5 mouse. Bar, 2.2 mm. (F) Ventral rib cage from a null sibling E18.5 mouse showing a bifurcated sternum. Bar, 2.2 mm. (G) Clavicles from E18.5 wild-type (top) and null (lower) siblings showing ventral curvature of the null clavicle. Bar, 0.9 mm.

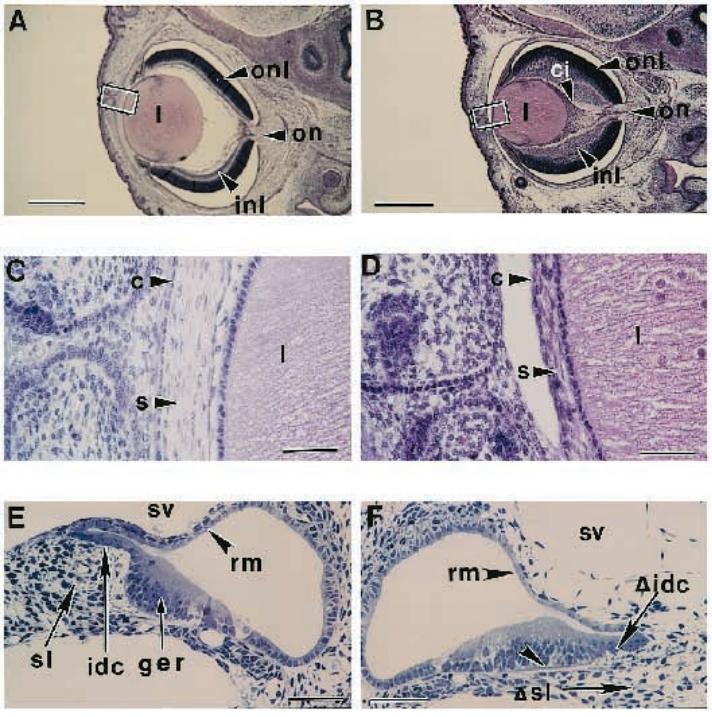

Fig. 5. Eye and inner ear defects from TGFβ2-null mice. (A) Transverse section from an E18.5 wild-type eye. Abbreviations: inl, inner neuroblastic layer; l, lens; on, optic nerve; onl, outer neuroblastic layer. Bar, 550 μm. (B) Transverse section from a null E18.5 eye showing an enlarged inner neuroblastic layer and a cellular infusion (ci). Bar, 550 μm. (C) Close-up view of the cornea from an E18.5 wild-type eye similar to the boxed region shown in A. Abbreviations: c, cornea; s, stroma. Bar, 55 μm. (D) Close-up view of the cornea from an E18.5 null mutant eye similar to the boxed region shown in B showing a reduced corneal stroma. Bar, 55 μm. (E) Toluidine blue-stained section from the basal turn of an E18.5 wild-type cochlea (right ear). Bar, 55 μm. (F) Toluidine blue-stained section from the basal turn of an E18.5 mutant cochlea (left ear) showing missing spiral limbus and interdental cells. Arrowhead indicates wider space between epithelial ridge and basilar membrane. Bar, 55 μm. Abbreviations: ger, greater epithelial ridge; idc, interdental cells; sl, spiral limbus; sv, scala vestibuli; Δsl, missing spiral limbus; rm, Reissner's membrane; Δidc, missing interdental cells.

in the tubular lumens and the enlarged renal pelvis of E18.5 null animals. Since the TGFβ2-null urogenital system was examined in only five males and five females, these findings are considered preliminary. Additional null mice must be examined to be certain of these trends.

Similarity to other TGFβ-related gene disruptions

The BMP7-null mouse shares some aspects of the TGFβ2-null phenotype with respect to the organs affected. These mice have skull defects, eye defects, kidney defects and perinatal lethality (Dudley et al., 1995; Luo et al., 1995). However, the specific details of these semblances are quite different. The BMP7 null skull has an abnormal basisphenoid bone, which was never seen in the TGFβ2-nulls. The BMP7 null mice displayed microophthalmia and anophthalmia, which were never observed in the TGFβ2-null mice. Finally, although nephrogenesis is severely affected around E12.5-E14.5, in the BMP7 null mice preliminary observations of female TGFβ2-null kidneys indicate that they are normal until around E 15.5.

The activin pathway has been explored by gene disruptions of both the ligands and the activin type II receptor. Ligand null mice manifested cleft palates and neonatal lethality resembling the TGFβ2-null mice (Matzuk et al., 1995a). However, these mice also lacked whiskers and incisors, which are present in the TGFβ2-null mice. The activin receptor null mice present with testicular, craniofacial and mandible defects (Matzuk et al., 1995b). However, they also have an abnormal Meckel's cartilage, eyelid defects and survival to adulthood which were never observed in the TGFβ2-null mice.

BMP-8B-deficient mice have two germ cell defects. During early puberty the germ cells in males show a proliferation and differentiation defect. Later in adult life, they show increased apoptosis of spermatocytes leading to sterility (Zhao et al., 1996). We have not yet histological examinations on hypoplastic testes from TGFβ2-null animals and consequently can not state whether the cellular events are similar in these two animals.

TGFβ2 phenotypes share features with Hox gene and retinoic acid deficiencies

Other mice with phenotypes similar to those of the TGFβ2-null mice are the offspring of vitamin A-deficient mice (Wilson et al., 1953). The retinoic acid receptor-αγ and βγ compound null animals possess nearly all of the developmental defects found in the TGFβ2-null mice (Lohnes et al., 1994; Mendelsohn et al., 1994, Lufkin et al., 1993). Many in vitro studies have reported the complex interplay between TGFβs and retinoic acid by showing that the addition of retinoic acid may induce or repress the expression of TGFβ depending on the cell type examined (Mummery et al., 1990; Glick et al., 1991; Abbott and Birnbaum, 1990; Taylor et al., 1995). Interestingly, the treatment of chicken embryos with retinoic acid caused a remarkably similar spectrum of heart defects to those described herein (Bouman et al., 1995). Given the widespread developmental expression of receptors for both TGFβ2 and retinoic acid, in addition to the remarkable similarity in knockout phenotypes, it is conceivable that the absence of TGFβ2 modifies the retinoic acid pathway in the null animals or that TGFβ2 is a proximal downstream effector for retinoic acid pathway as suggested by Glick et al. (1991).

The TGFβ2-null phenotypes can also be viewed in terms of its placement in the hierarchy of homeobox (Hox) gene regulation. A paradigm for this has been described in *Drosophila* in which the *decapentaplegic* gene product, a TGFβ family member, regulates the expression of *tinman*, a Hox gene (Frasch, 1995). Tinman expression is essential for visceral and cardiac muscle development in the fly (Bodmer, 1993). Some of the TGFβ2-knockout phenotypes are quite similar to those of mice with Hox gene ablations such as *Hox 1.5*, *pax-3* and *Mhox* (Chisaka and Capecchi, 1991; Epstein et al., 1991; Franz, 1989; Martin et al., 1995). There are a sizable number of Hox genes expressed in appropriate developmental regions

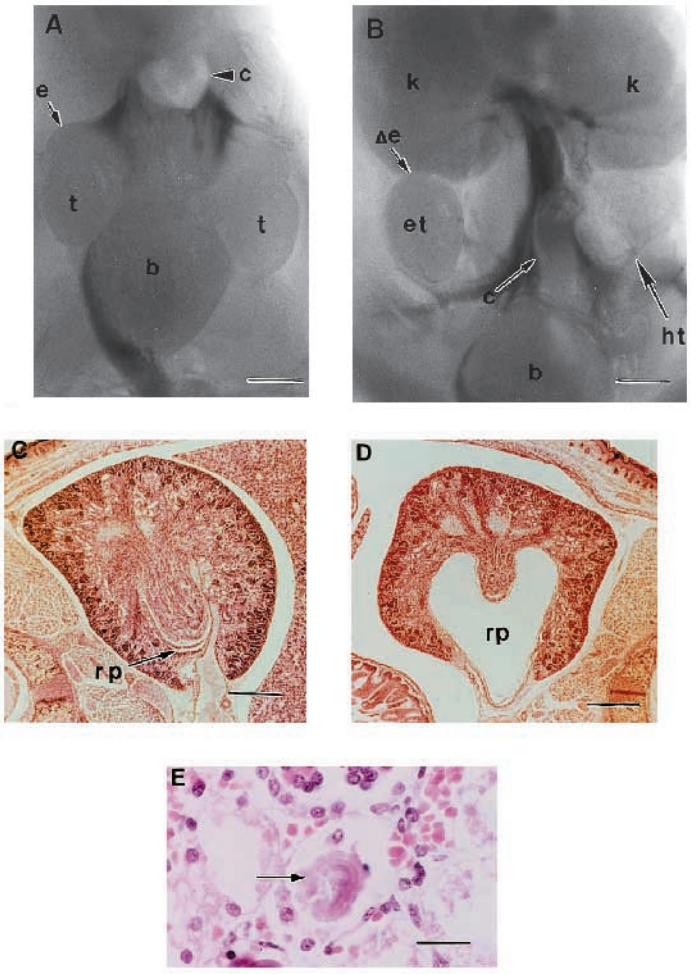

Fig. 6. Urogenital defects from TGFβ2 null mice. (A) Transverse Wilson section from a wild-type day E18.5 male showing normal genitalia. Kidneys not shown. Bar, 650 μm. (B) Transverse Wilson section from a null E18.5 male showing testicular ectopia, testicular hypoplasia and vas dysgenesis. Kidneys are present and appear normal. Bar, 650 μm. (C) Transverse Wilson section from a wild-type day E18.5 female showing normal kidney development. Bar, 300 μm. (D) Transverse Wilson section from a mutant day E18.5 female showing enlarged renal pelvis. Bar, 300 μm. (E) High-power view of dilated kidney tubules with degenerating epithelial cells and luminal protein casts. Bar, 3.7 μm. Abbreviations: b, bladder; c, colon; e, epididymis; Δe, deleted epididymis; et, ectopic testicle; ht, hypoplastic testicle; k, kidney; rp, renal pelvis.

of the embryo to be candidate genes for TGFβ2 regulation and vice versa. These phenotypic similarities between deficiencies in TGFβ2, retinoic acid receptors and several hox genes suggest common regulatory pathways.

Non-overlapping phenotypes of the three TGFβ knockout mice

The TGFβ2 knockout phenotype has no overlap with the published phenotype of the TGFβ-1 null mouse, which has an autoimmune-like inflammatory disease (Shull et al., 1992; Kulkarni et al., 1993; Diebold et al., 1995). Similarly, none of the TGFβ2 knockout phenotypes are found in the TGFβ3 knockout mouse, with one possible exception. Both the TGFβ2- and TGFβ3-deficient mice show postnatal defects in the conducting airways of the lungs. It is possible that reduced levels of surfactant expression could be responsible for this distal airway collapse (Clark et al., 1995). Kaartinen et al. (1995) proposed that lung morphogenesis is delayed in TGFβ3 knockout mice due to a defect in branching morphogenesis and respiratory epithelial cell differentiation. In contrast, the TGFβ2 deficient lungs do not appear to have a defect in either branching morphogenesis or epithelial cell differentiation.

Contrary to the fact that the TGFβ2 and TGFβ3 knockout mice both have cleft palates, the arrested developmental processes appear to have no similarities (Proetzel et al., 1995; Kaartinen et al., 1995). In the absence of TGFβ2, the palatal shelves fail to elevate and the penetrance is only 23%. In the TGFβ3 mutant, where cleft palate is at full penetrance, the palatal shelves elevate and become physically apposed, but the medial edge epithelia do not adhere to each other and remain persistent. Whereas, the TGFβ2 cleft palates were always extensive as seen in Fig. 3, the TGFβ3 cleft palates were of varying severity and do not always involve the soft palate (Proetzel et al., 1995). Therefore, the TGFβ knockout phenotypes are quite distinct, indicating a large number of functions that are not compensated by other members of the gene family.

Partial penetrance is common to some of the TGFβ2 knockout phenotypes, especially in the heart, palate, ribs and sternum. These differences may result from variability in genetic background, as seen in EGF receptor (Threadgill et al., 1995) and TGFβ1 (personal observations) knockout mice. The advantage of analyzing knockout phenotypes on a mixed background is that phenotypes with variable penetrance are good indicators of the presence of modifier genes. For example, we know that breeding the TGFβ1 knockout on a C57BL/6 background results in embryonic lethality, which interferes with the detection of the postnatal autoimmune-like inflammatory phenotype (unpublished observations). Consequently, the backcrossing of the targeted TGFβ2 allele onto other genetic backgrounds may alter not only the penetrance and expressivity of the mutant phenotypes described herein but may also provide the means to identify other genes that modify TGFβ2 function.

We thank Suhas Kallapur and Julian Molina for excellent suggestions and advice concerning the neonatal lethality; Susan Wert, Jeffrey Whitsett, Tom Korfhagen, Barbara O'Toole, Marian Miller, Jay Hoying and Nancy Paradies for their assistance with histology evaluations; Bert Wisse for the heart sectioning and screening; Jan Lens for heart photographs; and Bill Larsen for a critical reading of the manuscript. Support for this work was provided by National Institutes of Health grants HD26471 and HL41496 to T. D. and DC00119 to R. F.

REFERENCES

Abbott, B. D. and Birnbaum, L. S. (1990). Retinoic acid-induced alterations in the expression of growth factors in embryonic mouse palatal shelves. *Teratology* **42,** 597-610.

Barishak, Y. R. (1992). Embryology of the eye and its adnexae. *Dev. Ophthalmol*. **24,** 1-142.

Barnett, J. V., Moustakas, A., Lin, W., Wang, X. F., Lin, H. Y., Galper, J. B. and Maas, R. L. (1994). Cloning and developmental expression of the chick type II and type III TGF beta receptors. *Dev. Dyn.* **199,** 12-27.

Besson, W. T., Kirby, M. L., Van Mierop, L. H. and Teabeaut, J. R. (1986). Effects of the size of lesions of the cardiac neural crest at various embryonic ages on incidence and type of cardiac defects. *Circulation* **73,** 360-364.

Bodmer, R. (1993). The gene tinman is required for specification of the heart and visceral muscles in Drosophila. *Development* **118,** 719-729.

Bouman, H. G., Broekhuizen, M. L., Baasten, A. M., Gittenberger-de Groot, A. C. and Wenink, A. C. (1995). Spectrum of looping disturbances in stage 34 chicken hearts after retinoic acid treatment. *Anat. Rec.* **243,** 101-108.

Candia, A. F., Hu, J., Crosby, J., Lalley, P. A., Noden, D., Nadeau, J. H. and Wright, C. V. (1992). Mox-1 and Mox-2 define a novel homeobox gene subfamily and are differentially expressed during early mesodermal patterning in mouse embryos. *Development* **116,** 1123-1136.

Chisaka, O. and Capecchi, M. R. (1991). Regionally restricted developmental defects resulting from targeted disruption of the mouse homeobox gene hox-1.5. *Nature* **350,** 473-479.

Chomczynski, P. and Sacchi, N. (1987). Single-step method of RNA isolation by acid guanidinium thiocyanate-phenol-chloroform extraction. *Anal. Biochem.* **162,** 156-159.

Clark, J. C., Wert, S. E., Brachurski, C. J., Stahlman, M. T., Stripp, B. R., Weaver, T. E. and Whitsett, J. A. (1995). Targeted disruption of the surfactant B gene disrupts surfactant homeostasis, causing respiratory failure in newborn mice. *Proc. Natl. Acad. Sci. USA* **92,** 7794-7798.

Copp, A. J. (1995). Death before birth: clues from gene knockouts and mutations. *Trends Genet.* **11,** 87-93.

Couly, G. F., Coltey, P. M. and Le Douarin, N. M. (1993). The triple origin of skull in higher vertebrates: a study in quail-chick chimeras. *Development* **117,** 409-429.

Dickson, M. C., Slager, H. G., Duffie, E., Mummery, C. L. and Akhurst, R. J. (1993). RNA and protein localization of TGF beta 2 in the early mouse embryo suggest an involvement in cardiac development. *Development* **117,** 625-639.

Diebold, R. J., Eis, M. J., Yin, M., Ormsby, I., Boivin, G. P., Darrow, B. J., Saffitz, J. E. and Doetschman, T. (1995). Early-onset multifocal inflammation in the transforming growth factor beta 1-null mouse is lymphocyte mediated. *Proc. Natl. Acad. Sci. USA* **92,** 12215-12219.

Dudley, A. T., Lyons, K. M. and Robertson, E. J. (1995). A requirement for bone morphogenetic protein-7 during development of the mammalian kidney and eye. *Genes Dev.* **9,** 2795-2807.

Epstein, D. J., Vekemans, M. and Gros, P. (1991). Splotch (Sp2H), a mutation affecting development of the mouse neural tube, shows a deletion within the paired homeodomain of Pax-3. *Cell* **67,** 767-774.

Erickson, C. A. and Perris, R. (1993). The role of cell-cell and cell-matrix interactions in the morphogenesis of the neural crest. *Dev. Biol.* **159,** 60-74.

Flanders, K. C., Ludecke, G., Engels, S., Cissel, D. S.,Roberts, A. B., Kondaiah, P. Lafyatis, R., Sporn, M. B. and Unsicker, K. (1991). Localization and actions of transforming growth factor-beta s in the embryonic nervous system. *Development* **113,** 183-191.

Franz, T. (1989). Persistent truncus arteriosus in the Splotch mutant mouse. *Anat. Embryol.* **180,** 457-464.

Frasch, M. (1995). Induction of visceral and cardiac mesoderm by ectodermal Dpp in the early Drosophila embryo. *Nature* **374,** 464-467.

Frenz D. A., Galinovic-Schwartz, V., Liu W., Flanders, K. C. and Van De Water, T. R. (1991). Transforming growth factor 1 is an epithelial-derived signal peptide that inflences otic capsule formation. *Dev. Biol.* **153**, 324-336.

Glick, A. B., McCune, B. K., Abdulkarem, N., Flanders, K. C., Lumadue, J. A., Smith, J. M. and Sporn, M. B. (1991). Complex regulation of TGF beta expression by retinoic acid in the vitamin A-deficient rat. *Development* **111,** 1081-1086.

Hall, B. K. (1982). *Factors and Mechanisms Influencing Bone Growth*. (ed. A. S. Dixson and B. G. Sarnat). pp. 205-215. New York: A. R. Liss Inc.

Howard, M. J. and Gershon, M. D. (1993). Role of growth factors in catecholaminergic expression by neural crest cells: in vitro effects of transforming growth factor beta 1. *Dev. Dyn.* **196,** 1-10.

Kaartinen, V., Voncken, J. W., Shuler, C., Warburton, D., Bu, D., Heisterkamp, N. and Groffen, J. (1995). Abnormal lung development and cleft palate in mice lacking TGF-beta 3 indicates defects of epithelial-mesenchymal interaction. *Nature Genet.* **11,** 415-421.

Kingsley, D. M. (1994). The TGF-beta superfamily: new members, new receptors, and new genetic tests of function in different organisms. *Genes Dev.* **8,** 133-146.

Kulkarni, A. B., Huh, C. G., Becker, D., Geiser, A., Lyght, M., Flanders, K. C., Roberts, A. B., Sporn, M. B., Ward, J. M. and Karlsson, S. (1993). Transforming growth factor beta 1 null mutation in mice causes excessive inflammatory response and early death. *Proc. Natl. Acad. Sci. USA* **90,** 770-774.

Laird, P. W., Zijderveld, A., Linders, K., Rudnicki, M. A., Jaenisch, R. and Berns, A. (1991). Simplified mammalian DNA isolation procedure. *Nucl. Acids Res.* **19,** 4293

Le Douarin, N. M., Ziller, C. and Couly, G. F. (1993). Patterning of neural crest derivatives in the avian embryo: in vivo and in vitro studies. *Dev. Biol.* **159,** 24-49.

Le Lievre, C. S. and Le Douarin. N. M. (1975). Mesenchymal derivatives of the neural crest: analysis of chimaeric quail and chick embryos. *J. Embryol. Exp. Morph.* **34,** 125-154.

Leblanc, G. G., Holbert, T. E. and Darland, T. (1995). Role of the transforming growth factor-beta family in the expression of cranial neural crest-specific phenotypes. *J. Neurobiol.* **26,** 497-510.

Lohnes, D., Mark, M., Mendelsohn, C., Dolle, P., Dierich, A., Gorry, P., Gansmuller, A. and Chambon, P. (1994). Function of the retinoic acid receptors (RARs) during development (I). Craniofacial and skeletal abnormalities in RAR double mutants. *Development* **120,** 2723-2748.

Lufkin, T., Lohnes, D., Mark, M., Dierich, A., Gorry, P., Gaub, M. P., LeMeur, M. and Chambon, P. (1993). High postnatal lethality and testis degeneration in retinoic acid receptor alpha mutant mice. *Proc. Natl. Acad. Sci. USA* **90,** 7225-7229.

Luo, G., Hofmann, C., Bronckers, A. L. J. J., Sohocki, M., Bradley, A., and Karsenty, G. (1995). BMP-7 is an inducer of nephrogenesis, and is required for eye development and skeletal patterning. *Genes Dev.* **9,** 2808-2820.

Lutty, G. A., Merges, C., Threlkeld, A. B., Crone, S. and McLeod, D. S. (1993). Heterogeneity in localization of isoforms of TGF-beta in human retina, vitreous, and choroid. Invest. *Ophthalmol. Vis. Sci.* **34,** 477-487.

Manova, K., Paynton, B. V. and Bachvarova, R. F. (1992). Expression of activins and TGF beta 1 and beta 2 RNAs in early postimplantation mouse embryos and uterine decidua. *Mech. Dev.* **36,** 141-152.

Martin, J. F., Bradley, A. and Olson, E. N. (1995). The paired-like homeo box gene MHox is required for early events of skeletogenesis in multiple lineages. *Genes Dev.* **9,** 1237-1249.

Massagué, J. (1990). The transforming growth factor-beta family. *Ann. Rev. Cell Biol.* **6,** 597-641.

Matzuk, M. M., Kumar, T. R., Vassalli, A., Bickenbach, J. R., Roop, D. R., Jeanisch, R. and Bradley, A. (1995a). Functional analysis of activins during mammalian development. *Nature* **374,** 354-356.

Matzuk, M. M., Kumar, T. R. and Bradley, A. (1995b). Different phenotypes for mice deficient in either activins or activin receptor type II. *Nature* **374,** 356-360.

McLeod, M. J. (1980). Differential staining of cartilage and bone in whole mouse fetuses by alcian blue and alizarin red S. *Teratology* **22,** 299-301.

Mendelsohn, C., Lohnes, D., Decimo, D., Lufkin, T., LeMeur, M., Chambon, P. and Mark, M. (1994). Function of the retinoic acid receptors (RARs) during development (II). Multiple abnormalities at various stages of organogenesis in RAR double mutants. *Development* **120,** 2749-2771.

Millan, F. A., Denhez, F., Kondaiah, P. and Akhurst, R. J. (1991). Embryonic gene expression patterns of TGF beta 1, beta 2 and beta 3 suggest different developmental functions in vivo. *Development* **111,** 131-143.

Miller, D. A., Lee, A., Pelton, R. W., Chen, E. Y., Moses, H. L. and Derynck, R. (1989). Murine transforming growth factor-beta 2 cDNA sequence and expression in adult tissues and embryos. *Mol. Endocrinol.* **3,** 1108-1114.

Mummery, C. L., Slager, H., Kruijer, W., Feijen, A., Freund, E., Koornneef, I. and van den Eijnden-van Raaij, A. J. (1990). Expression of transforming growth factor beta 2 during the differentiation of murine embryonal carcinoma and embryonic stem cells. *Dev. Biol.* **137,** 161-170.

Nakasawa, K., Spicer, S. S. and Schulte, B .A. (1995). Ultrastructural localization of Na, K-ATPase in the gerbil cochlea. *J. Histochem. Cytochem.* **43,** 981-991.

Nichols, D. H. (1981). Neural crest formation in the head of the mouse embryo as observed using a new histological technique. *J. Embryol. Exp. Morph.* **64,** 105-120.

Nishida, K., Sotozono, C., Adachi, W., Yamamoto, S., Yokoi, N. and Kinoshita, S. (1995). Transforming growth factor-beta 1, -beta 2 and -beta 3 mRNA expression in human cornea. *Curr. Eye Res.* **14,** 235-241.

Noden, D. M. (1991). Vertebrate craniofacial development: the relation between ontogenetic process and morphological outcome. *Brain, Behavior Evol.* **38,**190-225.

Noden, D. M., Poelmann, R. E. and Gittenberger-de Groot, A. C. (1995). Cell origins and tissue boundaries during outflow tract development. *Trends Cardiovas. Med.* **5,** 69-75.

Paria, B. C., Jones, K. L., Flanders, K. C. and Dey, S. K. (1992). Localization and binding of transforming growth factor-beta isoforms in mouse preimplantation embryos and in delayed and activated blastocysts. *Dev. Biol.* **151,** 91-104.

Pasquale, L. R., Dorman-Pease, M. E., Lutty, G. A., Quigley, H. A. and Jampel, H. D. (1993). Immunolocalization of TGF-beta 1, TGF-beta 2, and TGF-beta 3 in the anterior segment of the human eye. *Invest. Ophthalmol. Vis. Sci.* **34,** 23-30.

Payne, R. M., Johnson, M. C., Grant, J. W. and Strauss, A. W. (1995). Toward a molecular understanding of congenital heart disease. *Circulation* **91,** 494-504.

Pei, Y. F. and Rhodin, J. A. (1970). The prenatal development of the mouse eye. *Anat. Rec.* **168,** 105-125.

Pelton, R. W., Dickinson, M. E., Moses, H. L. and Hogan, B. L. (1990). In situ hybridization analysis of TGF beta 3 RNA expression during mouse development: comparative studies with TGF beta 1 and beta 2. *Development* **110,** 609-620.

Pelton, R. W., Saxena, B., Jones, M., Moses, H. L. and Gold, L. I. (1991). Immunohistochemical localization of TGF beta 1, TGF beta 2, and TGF beta 3 in the mouse embryo: expression patterns suggest multiple roles during embryonic development. *J. Cell Biol.* **115,** 1091-1105.

Polikar, R., Burger, A. G., Scherrer, U. and Nicod, P. (1993). The thyroid and the heart. *Circulation* **87,** 1435-1441.

Proetzel, G., Pawlowski, S. A., Wiles, M. V., Yin, M., Boivin, G. P., Howles, P. N., Ding, J., Ferguson, M. W. and Doetschman, T. (1995). Transforming growth factor-beta 3 is required for secondary palate fusion. *Nature Genet.* **11,** 409-414.

Roberts, A. B., Anzano, M. A., Lamb, L. C., Smith, J. M. and Sporn, M. B. (1981). New class of transforming growth factor: isolation from non-neoplastic tissues. *Proc. Natl. Acad. Sci.* USA **78,** 5339-5343.

Rogers, S. L., Gegick, P. J., Alexander, S. M. and McGuire, P.G. (1992). Transforming growth factor-beta alters differentiation in cultures of avian neural crest-derived cells: effects on cell morphology, proliferation, fibronectin expression, and melanogenesis. *Dev. Biol.* **151,** 192-203.

Rosenquist, T. H. and Beall, A. C. (1990). Elastogenic cells in the developing cardiovascular system. Smooth muscle, nonmuscle, and cardiac neural crest. *Ann. NY Acad. Sci.* **588,** 106-119.

Rossant, J. (1996). Mouse mutants and cardiac development: new molecular insights into cardiogenesis. *Circ. Res.* **78,** 349-353.

Sambrook, J., Fritch, E. F. and Maniatis, T. (1989). *Molecular Cloning: A Laboratory Manuel*, 2nd Edition. Cold Springs Harbor, New York: Cold Spring Harbor Press.

Schmid, P., Cox, D., Bilbe, G., Maier, R. and McMaster, G. K. (1991). Differential expression of TGF beta 1, beta 2 and beta 3 genes during mouse embryogenesis. *Development* **111,** 117-130.

Shull, M. M., Ormsby, I., Kier, A. B., Pawlowski, S., Diebold, R. J., Yin, M., Allen, R., Sidman, C., Proetzel, G., Calvin, D., Annunziata, N. and Doetschman, T. (1992). Targeted disruption of the mouse transforming growth factor-beta 1 gene results in multifocal inflammatory disease. *Nature* **359,** 693-699.

Slager, H. G., Lawson, K. A., van den Eijnden-van Raaij, A. J., de Laat, S. W. and Mummery, C. L. (1991). Differential localization of TGF-beta 2 in mouse preimplantation and early postimplantation development. *Dev. Biol.* **145,** 205-218.

Sporn, M. B., Roberts, A. B., Wakefield, L. M. and de Crombrugghe, B. (1987). Some recent advances in the chemistry and biology of transforming growth factor-beta. *J. Cell Biol.* **105,** 1039-1045.

Sucov, H. M., Dyson, E., Gumeringer, C. L., Price, J., Chien, K. R. and Evans, R. M. (1994). RXR alpha mutant mice establish a genetic basis for vitamin A signaling in heart morphogenesis. *Genes Dev.* **8,** 1007-1018.

Taylor, L. E., Bennett, G. D. and Finnell, R. H. (1995). Altered gene expression in murine branchial arches following in utero exposure to retinoic acid. *Journal of Craniofacial Genetics and Dev. Biol.* **15,** 13-25.

Threadgill, D. W., Dlugosz, A. A., Hansen, L. A., Tennenbaum, T., Lichti, U., Yee, D., LaMantia, C., Mourton, T., Herrup, K., Harris, R. C. and et

al. (1995). Targeted disruption of mouse EGF receptor: effect of genetic background on mutant phenotype. *Science* **269,** 230-234.

Topouzis, S., and Majesky, M. W. (1996). Smooth muscle lineage diversity in the chick. *Dev. Biol*. **178,** 430-445.

Tripathi, B. J., Tripathi, R. C., Livingston, A. M. and Borisuth, N. S. (1991). The role of growth factors in the embryogenesis and differentiation of the eye. *Am. J. Anat.* **192,** 442-471.

Van De Water T. R. (1991). Epithelial-mesenchymal tissue interactions effect upon development of the inner ear (abstract). *Anat. Rec.* **199,** 260.

Wilson, J., Roth, C. B. and Warkarny, J. (1953). An analysis of malformations induced by maternal vitamin A deficiency. Effects of restoration of vitamin A at various times during gestation. *Am. J. Anat.* **92,** 189-217.

Zuo J., Curtis L. M., Yao X., Ten Cate W. J. F., et al. (1995). Expression of Na, K-ATPase α and β isoforms in the neonatal rat cochlea. *Acta Otolaryngol (Stockh)* **115**, 497-503.

Zhao, G.-Q., Deng, K., Labosky, P. A., Liaw, L. and Hogan, B. L. M. (1996). The gene encoding bone morphogenetic protein 8B is required for the initiation and maintenance of spermatogenesis in the mouse. *Genes Dev.* **10,** 1657-1669.

(Accepted 17 April 1997)